




Phase Transformation of Hercynite During the Oxidative Roasting Process

XIAOBIN LI,¹ HONGYANG WANG ^{1,2,3} QIUSHENG ZHOU,^{1,4}
TIANGUI QI,¹ GUIHUA LIU,¹ and ZHIHONG PENG¹

1.—School of Metallurgy and Environment, Central South University, Changsha 410083, Hunan, China. 2.—School of Resources and Environmental Engineering, Wuhan University of Technology, Wuhan 430070, China. 3.—e-mail: hywang3@whut.edu.cn. 4.—e-mail: qszhou@csu.edu.cn

Converting the aluminum in hercynite into a readily soluble state in alkali solution is significant for extracting alumina from hercynite. Thermodynamic analysis shows that the aluminum in hercynite is insoluble in alkali solution and that it can be chemically separated from iron through oxidative roasting. X-ray diffraction combined with x-ray photoelectron spectroscopy analysis indicates that, during oxidative roasting, hercynite first decomposes into γ - Al_2O_3 and Fe_3O_4 with lattice distortion. With increasing temperature, the former subsequently converts into α - Al_2O_3 while the latter into γ - Fe_2O_3 followed by α - Fe_2O_3 . Hercynite can be completely converted into alumina and iron oxides through treatment at > 1173 K for 20 min. Alumina in the oxidized hercynite obtained at 1173 K to 1373 K can be efficiently digested by the Bayer digestion at 513 K and 533 K, with an alumina digestion ratio of $\sim 96\%$ and $\sim 98\%$, respectively. This work lays the foundation for alumina extraction from hercynite.

INTRODUCTION

A large amount of coal-based solid waste, including coal gangue, circulating fluidized bed slag and coal fly ash, has to be stockpiled owing to low utilization.^{1–3} To improve the use of coal-based solid waste at a large scale, scholars should increasingly focus on the production of building materials, such as brick,⁴ cement⁵ and pottery.⁶ However, these approaches cannot absorb a great amount of such minerals, because the building materials have limited transportation distance owing to the low value. Moreover, some of the minerals are rich in alumina and may be potential candidates for producing alumina especially in China. In 2018, the alumina yield reached 72 million tons in China, but the bauxite reserve is about 1 billion tons and bauxite production is 70 million tons per year.⁷ According to statistics,⁸ 100 billion tons of high alumina coal (HAC) has Al_2O_3 content in its ash of 38–51%, which is mainly distributed in Northern China, including Xinjiang Autonomous Region, Inner Mongolia and Shanxi Province. About 100–125 million tons of solid HAC waste is generated

annually. Therefore, exploring a new method for alumina extraction from such solid waste is of great importance in China.

In the last decade, several attempts were made to recover alumina from coal-based solid waste with high alumina content through acid leaching and sintering. In acid leaching, alumina is extracted with sulfuric acid or hydrochloric acid from minerals activated mechanically⁹ or thermally.¹⁰ The leached residue is used to produce silicon-containing materials.¹¹ This process has limited application because of equipment corrosion, difficulty in iron removal from solution and wastewater generation. In sintering, which includes lime sintering and lime-soda sintering, alumina is converted into $12\text{CaO}\cdot 7\text{Al}_2\text{O}_3$ or NaAlO_2 while silica into $2\text{CaO}\cdot \text{SiO}_2$.^{12–14} This process encounters the issue of massive leached residue (> 1.9 – 3.6 t/t- Al_2O_3).

Alkali leaching of silica from activation-roasted high-silica bauxite can increase the mass ratio of alumina to silica (A/S) in the residue and favors alumina extraction by the Bayer process.^{15–17} However, the formation of $3\text{Al}_2\text{O}_3\cdot 2\text{SiO}_2$ Al–Si spinel during roasting kaolinite alone causes a low silica

leaching ratio.^{18,19} As such, this approach is unsuitable for treating coal-based solid waste with A/S of ~ 1.0 to obtain a decent material ($A/S > 8.0$) for the Bayer process.

To realize the efficient separation of silica and alumina in coal-based solid waste, the authors introduce a new method for a reducing roasting-alkali leaching process (RRALP).^{19–21} In reduction roasting with hematite, full chemical disconnection of silica and alumina in aluminosilicates, including kaolinite, metakaolinite and mullite, can be obtained by forming hercynite and free silica in the forms of quartz solid solution and cristobalite solid solution. Free silica in the reduction roasted product is removed by alkali leaching under atmospheric pressure. Hercynite is stable and enriched in leaching residue. However, alumina extraction from hercynite has not been reported yet. Our trial experiments show that aluminum in hercynite cannot be dissolved through Bayer digestion even at 533 K for 60 min, because well-crystalline hercynite spinel is generally considered alkali resistant. Therefore, aluminum in hercynite must be converted into a readily soluble state prior to Bayer digestion. To our knowledge, research on the conversion of hercynite during oxidative roasting is limited. Jastrzębska et al.^{22,23} reported that only about half of the hercynite prepared by melting in an arc furnace can be decomposed into iron and alumina oxides by roasting at 1273 K for 36 h in air. Given that the conditions of forming hercynite by roasting in the present study differ from those of melting, the decomposition behavior of hercynite may differ from that reported because of differences in the specific structure and chemical properties. Hence, to activate aluminum in hercynite for Bayer digestion, the present study investigated the phase transformations of hercynite during oxidative roasting together with Bayer digestion of alumina.

EXPERIMENTAL

Materials and Methods

Hercynite was obtained by alkali leaching of silica in clinker, which was prepared by reductively roasting a mixture of kaolin, hematite and coal powder with $\text{Fe}_2\text{O}_3/\text{Al}_2\text{O}_3/\text{C}$ at a molar ratio of 1.2:2.0:1.2 at 1373 K for 60 min.^{19,20} The chemical compositions and XRD patterns of kaolin, clinker and hercynite are shown in supplementary Table SI and Figure S1. Sodium aluminate solution was obtained by dissolving analytical-grade aluminum hydroxide into hot sodium hydroxide solution.

The thermo-gravimetric analysis (TGA) and differential scanning calorimetry (DSC) of hercynite were carried out by thermal analyzer (SDTQ600, TA, USA) with air velocity of 100 mL/min and heating rate of 10 K/min from 300 K to 1373 K. Phase analysis was performed on powder using an x-ray diffractometer (XRD, TTR-III, Rigaku Corp., Japan) with Cu $K\alpha$ radiation ($\lambda = 1.5406 \text{ \AA}$) and x-

ray photoelectron spectroscopy (XPS, Thermo ESCALAB 250XI).

EDTA titrimetric volumetry was used to measure the content of Al_2O_3 . The alumina digestion ratio $\eta(\text{Al}_2\text{O}_3)$ was calculated by Formula (1).

$$\eta(\text{Al}_2\text{O}_3) = \frac{Q_a m_a - Q_b m_b}{Q_a m_a} \times 100\% \quad (1)$$

where m represents the alumina content in mass%, Q is the mass, and subscript a and b denote the raw material and residue, respectively.

Experimental Procedure

In brief, 5 g of hercynite was spread evenly in a 100-mL corundum crucible, which was heated in a thermostatic muffle furnace (SX-5-12, Changsha Dianlu Co., Ltd., China) with air velocity of 600 mL/min at a preset temperature for different durations. The crucible was then removed from the furnace and cooled in air to room temperature.

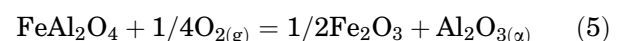
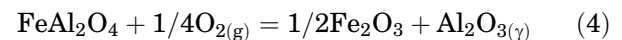
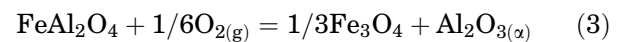
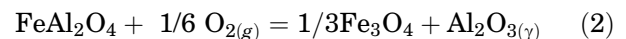
The alumina digestion experiments were performed in an autoclave (GS-0.25, Weihai Dingda Chemical Machinery Co., Ltd, China). About 20 g of oxidized hercynite and 100 mL of sodium aluminate solution ($\rho(\text{Na}_2\text{O}_k) = 230 \text{ g L}^{-1}$, $\alpha_k = 3$, Na_2O_k denotes caustic alkali in Na_2O , and α_k is the molar ratio of Na_2O_k to Al_2O_3 in the solution) were mixed, placed in the autoclave and heated. After the reaction, the autoclave was immediately cooled by using tap water. The digested residue (red mud) was obtained by filtration.

RESULTS AND DISCUSSION

Thermodynamic Analysis

Oxidative Roasting

Hercynite has a normal spinel structure, where one-eighth of the tetrahedral sites and one half of the octahedral sites are occupied by Fe^{2+} and Al^{3+} , respectively. During oxidative roasting, Fe^{2+} would be oxidized into Fe^{3+} , resulting in decomposition of hercynite. The possible reactions are listed in Eqs. 2, 3, 4, and 5. The stoichiometric coefficient of FeAl_2O_4 was normalized as 1 for convenient comparison. The relationships between standard Gibbs free energy change $\Delta_r G^\ominus$ and temperature T were calculated, in which thermodynamic data were derived from the literature.²⁴ The calculation results are plotted in Fig. 1.



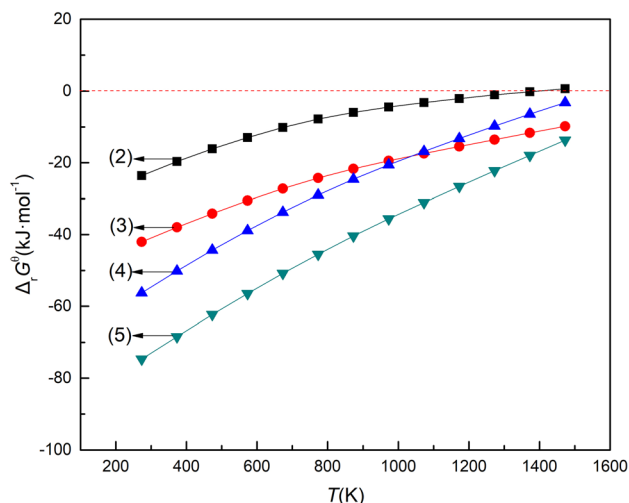


Fig. 1. Relationships between $\Delta_r G^\ominus$ and T for Eqs. 2, 3, 4, and 5.

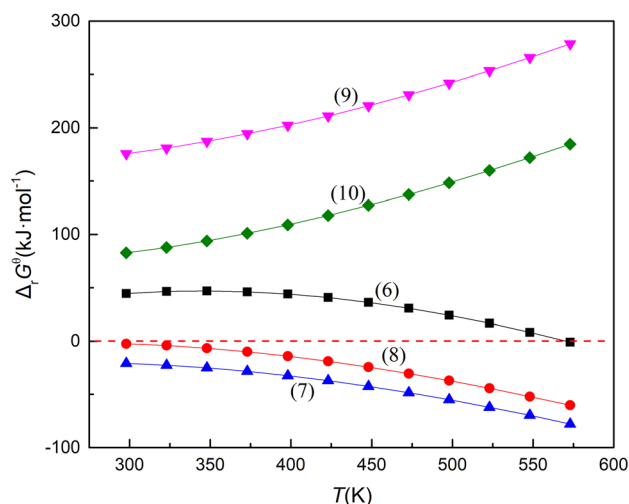


Fig. 2. Relationships between $\Delta_r G^\ominus$ and T for Eqs. 6, 7, 8, 9, and 10.

As shown in Fig. 1, all $\Delta_r G^\ominus$ values for Eqs. 2, 3, 4, and 5 are negative at < 1373 K but increase with rising roasting temperature. Hercynite can decompose into separate alumina and iron oxides, namely magnetite [Eqs. 2 and 3] or hematite [Eqs. 4 and 5]. Furthermore, the decomposition of hercynite proceeds more likely through Eqs. 4 and 5 because of their more negative values of $\Delta_r G^\ominus$ than in Eqs. 2 and 3, generating hematite and alumina.

Alumina Digestion

The dissolution of aluminum in hercynite and its oxidized products during Bayer digestion was thermodynamically analyzed. The possible reactions are listed in Eqs. 6, 7, 8, 9, and 10. For contrastive analysis, the stoichiometric coefficient of OH^- was normalized as 2. Based on the thermodynamic data

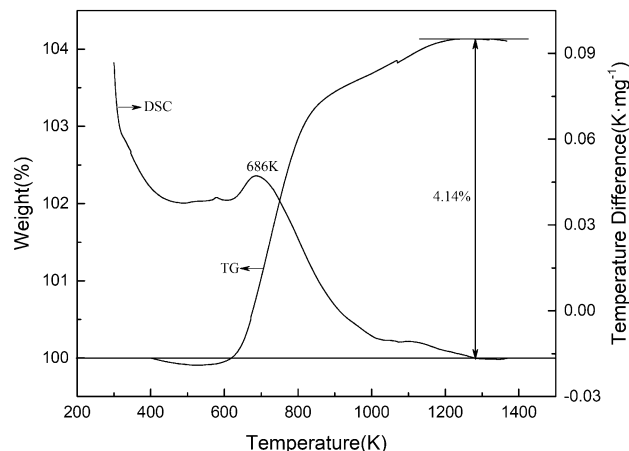


Fig. 3. TG-DSC curves of hercynite.

from the literature,^{25,26} the relationships between the standard Gibbs free energy change $\Delta_r G^\ominus$ and temperature T for these reactions were calculated (Fig. 2).

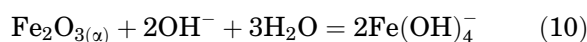
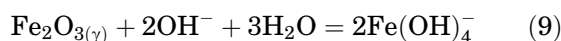
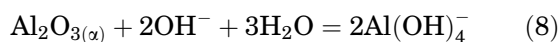
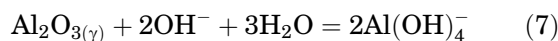
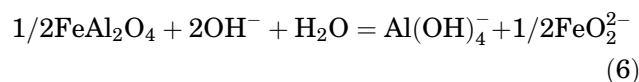


Figure 2 shows that hercynite cannot react with alkali solution in Bayer digestion because of the positive $\Delta_r G^\ominus$ value of Eq. 6 at < 573 K. $\gamma\text{-Al}_2\text{O}_3$ and $\alpha\text{-Al}_2\text{O}_3$ in the oxidation roasted product of hercynite can be dissolved in alkali solution because of the negative $\Delta_r G^\ominus$ values of Eqs. 7 and 8, while $\gamma\text{-Fe}_2\text{O}_3$ and $\alpha\text{-Fe}_2\text{O}_3$ cannot be dissolved because of the positive $\Delta_r G^\ominus$ values of Eqs. 9 and 10. Moreover, increasing the digestion temperature favors the Bayer digestion of alumina from the oxidation roasted product. Therefore, pre-oxidative roasting is beneficial to extract alumina from hercynite by Bayer digestion.

Oxidative Roasting of Hercynite

TG-DSC Analysis

The results of thermodynamic analysis indicate that the complete decomposition of hercynite by oxidative roasting is the premise of alumina extraction by Bayer digestion. As shown in Fig. 3 of the TG-DSC curves for hercynite, the sharp increase in the TG curve implies the rapid oxidizing reaction of

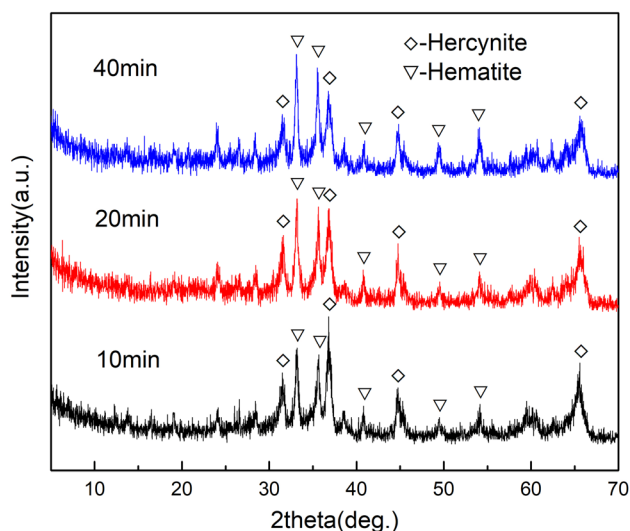


Fig. 4. XRD patterns of oxidized products prepared by roasting hercynite at 1073 K.

hercynite at 600 K to 1273 K, consistent with the appearance of the exothermic peak in the DSC curve at 686 K. Furthermore, the weight increases by 4.14% in the TG curve at 1273 K, which is close to that of the complete decomposition of hercynite into hematite and alumina at 4.42%.

XRD Analysis

The oxidized products of hercynite at different temperatures for various durations were analyzed by XRD to verify the results of thermodynamic and TG-DSC analyses.

As shown in Fig. 4, the diffraction apex of hercynite at 2 theta of 36.9° decreases significantly with roasting duration; the intensities are 761, 574 and 438 with 10 min, 20 min and 40 min, respectively. Compared with Fig. S1(c), Fig. 4 shows the typical diffraction peaks of hematite in the XRD patterns of the oxidized hercynite at 1073 K. With prolonged duration, the diffraction apices of hematite increase, whereas the diffraction apices of hercynite decrease. These results imply that the hercynite can decompose into hematite and amorphous alumina in oxidative roasting. The decomposition is not sufficiently rapid at 1073 K because a considerable amount of hercynite still exists in the product even after roasting for 40 min.

The effect of roasting temperature was studied to accelerate the decomposition. Figure 5 shows the XRD patterns of the oxidized products obtained by roasting hercynite for 20 min at different temperatures. The hercynite diffraction apices decrease with increasing roasting temperature from 573 K to 1073 K, and the diffraction peaks disappear at ≥ 1173 K. This finding indicates that raising the temperature benefits the decomposition. The diffraction peaks of α - Fe_2O_3 in the oxidized products obtained at ≥ 973 K are detected, while those of α -

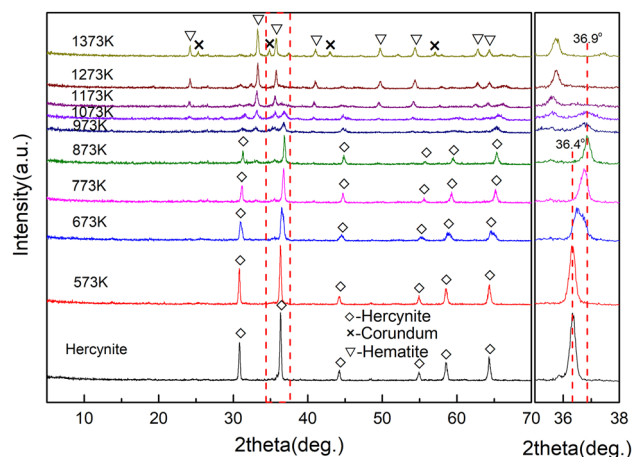


Fig. 5. XRD patterns of oxidized products prepared by roasting hercynite at different temperatures for 20 min. Right inset: amplified zone at $35\text{--}38^\circ$.

Al_2O_3 can only be detected in the product obtained at 1373 K. That is, the ultimate decomposition products of hercynite are α - Fe_2O_3 and α - Al_2O_3 derived from oxidative roasting, consistent with the results of thermodynamic analysis. Moreover, alumina in amorphous state maybe exist in the oxidized products obtained at 573–1273 K because of the decomposition of hercynite. This phenomenon will be subsequently discussed.

The amplified zone at $35^\circ\text{--}38^\circ$ was inserted in the right in Fig. 5. The 2 theta corresponding to the (311) direction in hercynite gradually increases with increasing temperature, shifting from 36.4° in oxidized hercynite to 36.9° in oxidized products obtained at 573 K to 873 K. The diffraction apex of hercynite decreases. The lattice parameter decreases from 8.249 Å for hercynite to 8.206 Å, 8.174 Å, 8.104 Å and 8.055 Å at 573 K, 673 K, 773 K and 873 K, respectively, indicating that the lattice distortion of hercynite occurs even at 573 K and aggravates with increasing temperature. Hence, at 973 K to 1073 K, the diffraction apex of hercynite decreases dramatically with the appearance of α - Fe_2O_3 diffraction peaks, suggesting the nearly utmost distortion.

XPS Analysis

Hercynite and its oxidized products obtained at ≤ 1373 K were analyzed by XPS to ascertain the amorphous phases (Fig. 6). As shown in Fig. 6a, γ - Al_2O_3 and FeAl_2O_4 are detected in the oxidized hercynite at 573 K. The content of γ - Al_2O_3 in oxidized products increases with temperature rising from 573 K to 1073 K; meanwhile, that of FeAl_2O_4 decreases. Hence, elevated temperature benefits the decomposition of FeAl_2O_4 . Moreover, γ - Al_2O_3 and α - Al_2O_3 are the main Al-containing phases in the oxidized hercynite at 1173 K. Increasing temperature promotes the conversion of γ - Al_2O_3 into α - Al_2O_3 . As shown in Fig. 6b, the content of FeAl_2O_4

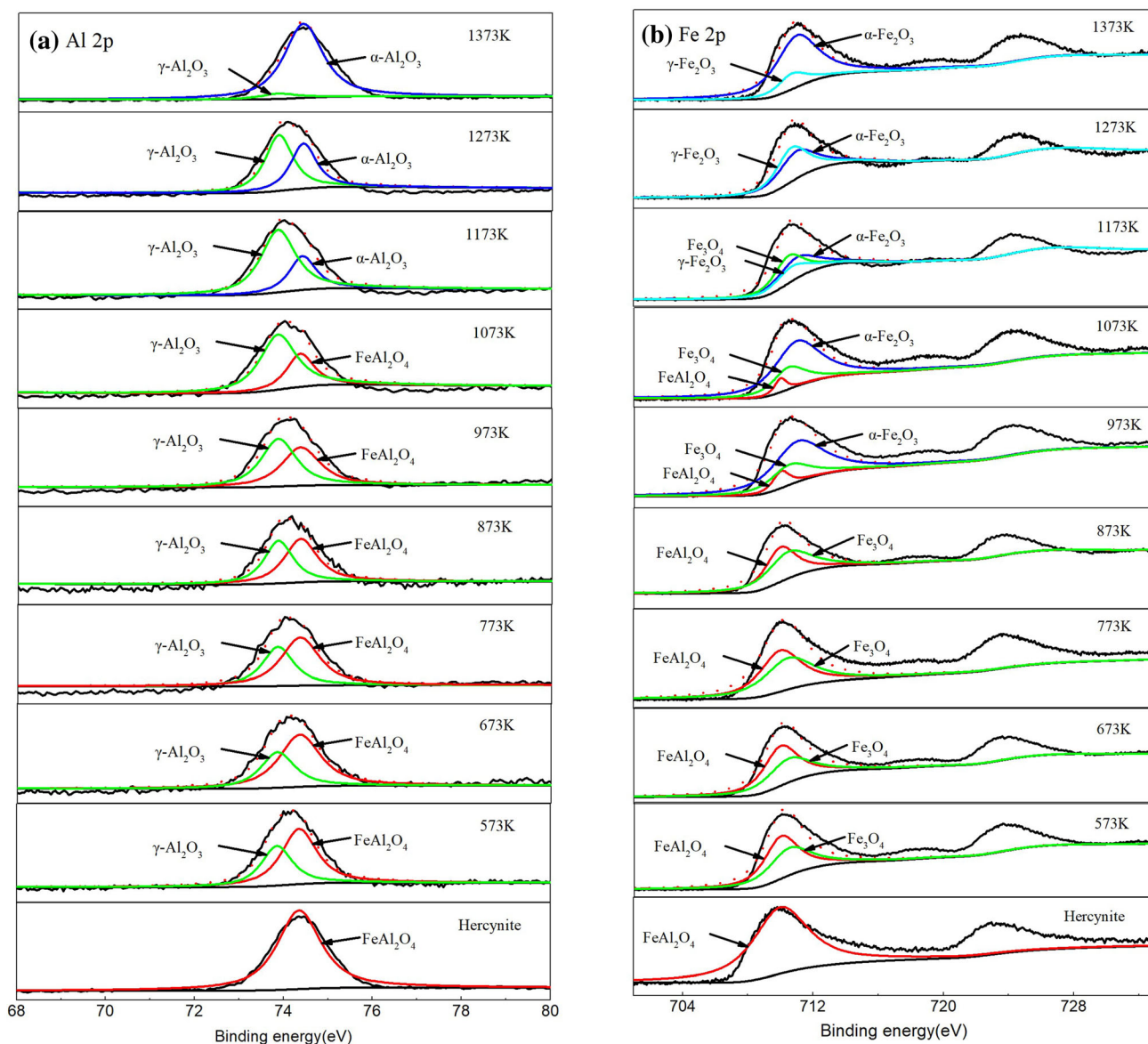


Fig. 6. Al 2p (a) and Fe 2p (b) XPS spectra of hercynite and its oxidized products at different temperatures for 20 min.

in the oxidized products decreases as the temperature increases from 573 K to 1073 K and disappears at ≥ 1173 K. Fe_3O_4 is the only iron oxide in the oxidized products at 573–873 K, while $\alpha\text{-Fe}_2\text{O}_3$ and $\gamma\text{-Fe}_2\text{O}_3$ appear in oxidized products at ≥ 973 K. As such, iron in hercynite first converts into Fe_3O_4 during oxidative roasting and then transforms into $\gamma\text{-Fe}_2\text{O}_3$ followed by $\alpha\text{-Fe}_2\text{O}_3$.

The decomposition of hercynite was verified by combining XRD and XPS analyses. During oxidative roasting, hercynite first converts into $\gamma\text{-Al}_2\text{O}_3$ and Fe_3O_4 at 573 K with lattice distortion. When the roasting temperature reaches > 973 K, $\gamma\text{-Al}_2\text{O}_3$ gradually develops into $\alpha\text{-Al}_2\text{O}_3$, while Fe_3O_4 into $\gamma\text{-Fe}_2\text{O}_3$ followed by $\alpha\text{-Fe}_2\text{O}_3$. This evolution law of hercynite during roasting is in agreement with that reported by Jastrzębska et al.²² However, hercynite

in this work decomposes rapidly because of the obvious differences in the synthesis conditions.

Alumina Extraction from Oxidized Hercynite

Hercynite and its oxidized products obtained at 873–1373 K for 20 min were digested in sodium aluminate solution at 513 K and 533 K, respectively (Fig. 7). The alumina digestion ratio of 2.55% in hercynite at 533 K for 60 min verifies that hercynite is insoluble in alkali solution, as discussed in thermodynamic analysis. Moreover, the alumina digestion ratio in the oxidized hercynite increases sharply as the oxidative roasting temperature increases from 873 K to 1173 K and subsequently rises slightly from 1273 K to 1373 K. The maximum alumina digestion ratio reaches $\sim 96\%$ and $\sim 98\%$ at 513 K and 533 K, respectively. Based on the

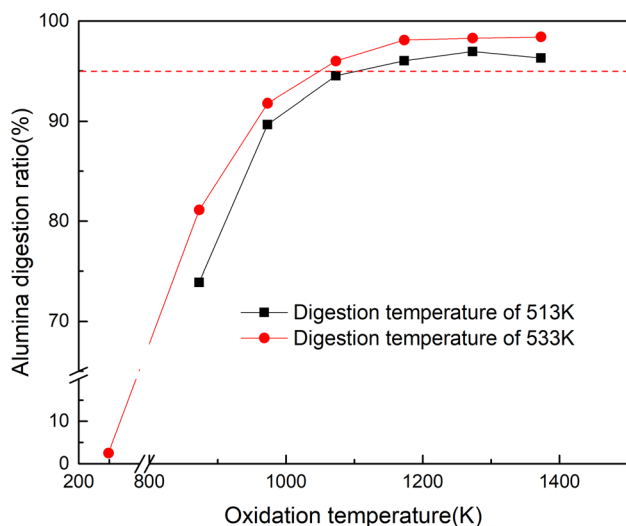


Fig. 7. Digestion results of hercynite and its oxidized products at different temperatures for 20 min. Digestion conditions: 60 min, $\rho(\text{Na}_2\text{O}_k) = 230 \text{ g L}^{-1}$, $\alpha_k = 3$, solid/liquid of 20 g/100 mL.

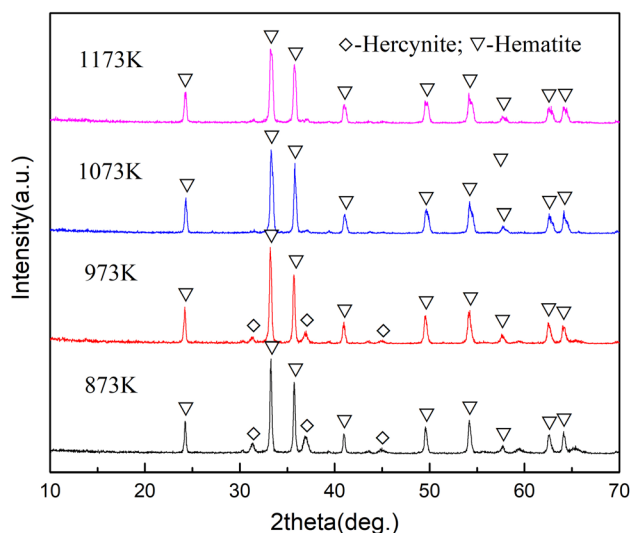


Fig. 8. XRD patterns of red mud of oxidized hercynite at 873–1173 K. Digestion conditions: 533 K, 60 min, $\rho(\text{Na}_2\text{O}_k) = 230 \text{ g L}^{-1}$, $\alpha_k = 3$, solid/liquid of 20 g/100 mL.

results of XRD and XPS spectral analyses, the full decomposition of hercynite is the premise of alumina extraction by Bayer digestion. Overall, alumina from the decomposition of hercynite can be efficiently digested at 533 K.

Red mud obtained at 533 K was further analyzed by XRD to verify the abovementioned discussion. As shown in Fig. 8, hercynite can be found in the red mud of oxidized hercynite at 873 K and 973 K. Hence, hercynite is stable in sodium aluminate solution at 533 K and leads to the low digestion ratio of alumina. However, only hematite is present in the red mud of oxidized hercynite at 1073 K and 1173 K. Thus, an appropriate oxidative roasting

temperature is needed for alumina extraction from hercynite by Bayer digestion.

CONCLUSION

- (1) Thermodynamic analysis and experiments indicate that aluminum in hercynite cannot be dissolved in the Bayer digestion at elevated temperature.
- (2) With oxidative roasting temperature increasing, hercynite decomposes into $\gamma\text{-Al}_2\text{O}_3$ and Fe_3O_4 with lattice distortion at 573 K; the former subsequently converts into $\alpha\text{-Al}_2\text{O}_3$ at 1173 K, while the latter into $\gamma\text{-Fe}_2\text{O}_3$ followed by $\alpha\text{-Fe}_2\text{O}_3$ at $\geq 973 \text{ K}$. The decomposition completes at $\geq 1173 \text{ K}$ for 20 min.
- (3) The full decomposition of hercynite is the premise of alumina extraction by Bayer digestion, and the alumina from the decomposition of hercynite can be efficiently digested at 533 K.

ACKNOWLEDGEMENTS

This work was financially supported by the National Natural Science Foundation of China (51604309) and China Postdoctoral Science Foundation (2019M662733).

ELECTRONIC SUPPLEMENTARY MATERIAL

The online version of this article (<https://doi.org/10.1007/s11837-020-04215-3>) contains supplementary material, which is available to authorized users.

REFERENCES

1. J.Y. Li and J.M. Wang, *J. Cleaner Prod.* 117946 (2019).
2. R.S. Blissett and N.A. Rowson, *Fuel* 97, 1 (2010).
3. A. Kumar, S.R. Samadder, and S.P. Elumalai, *JOM* 68, 2413 (2016).
4. Y. Taha, M. Benzaazoua, R. Hakkou, and M. Mansori, *Miner. Eng.* 107, 123 (2017).
5. M.P. Kuz'min, L.M. Larionov, V.V. Kondratiev, M.Y. Kuz'mina, V.G. Grigoriev, and A.S. Kuz'mina, *Constr. Build. Mater.* 179, 117 (2018).
6. Q.K. Lü, X.F. Dong, Z.W. Zhu, and Y.C. Dong, *J. Hazard. Mater.* 273, 136 (2014).
7. Mineral commodity summaries: bauxite and alumina (United States Geological Survey, 2019) <https://minerals.usgs.gov/minerals/pubs/commodity/bauxite/mcs-2019-bauxi.pdf>.
8. F.H. Li and Y.T. Fang, *Energy Fuels* 30, 2925 (2016).
9. Y.X. Guo, K.Z. Yan, L. Cui, and F.Q. Cheng, *Powder Technol.* 302, 33 (2016).
10. L. Dong, X.X. Liang, Q. Song, G.W. Gao, L.H. Song, Y.F. Shu, and X.Q. Shu, *J. Therm. Sci.* 26, 570 (2017).
11. J. Xiao, F. Li, Q. Zhong, H. Bao, B. Wang, J. Huang, and Y. Zhang, *Hydrometallurgy* 155, 118 (2015).

12. J. Ding, S.H. Ma, S. Shen, Z.L. Xie, S.L. Zheng, and Y. Zhang, *Waste Manage.* 60, 375 (2017).
13. Z.T. Yao, M.S. Xia, P.K. Sarker, and T. Chen, *Fuel* 120, 74 (2014).
14. G.Z. Lu, T.A. Zhang, W. Feng, W.G. Zhang, Y.X. Wang, Z.W. Zhang, L. Wang, Y. Liu, and Z.H. Dou, *JOM* 71, 499 (2019).
15. G.Z. Qiu, T. Jiang, G.H. Li, X.H. Fan, and Z.C. Huang, *Scand. J. Metall.* 33, 121 (2004).
16. V.L. Rayzman, A.V. Aturin, I.Z. Pevzner, V.M. Sizyakov, L.P. Ni, and I.K. Filipovich, *JOM* 55, 47 (2003).
17. P. Smith, *Hydrometallurgy* 98, 162 (2009).
18. A.K. Chakraborty, *J. Mater. Sci.* 27, 2075 (1992).
19. X.B. Li, H.Y. Wang, Q.S. Zhou, T.G. Qi, G.H. Liu, Z.H. Peng, and Y.L. Wang, *Trans. Nonferrous Met. Soc. China* 29, 416 (2019).
20. X.B. Li, H.Y. Wang, Q.S. Zhou, T.G. Qi, G.H. Liu, Z.H. Peng, and Y.L. Wang, *Trans. Nonferrous Met. Soc. China* 29, 186 (2019).
21. X.B. Li, H.Y. Wang, Q.S. Zhou, T.G. Qi, G.H. Liu, and Z.H. Peng, *Waste Manage.* 87, 798 (2019).
22. I. Jastrzębska, J. Szczerba, A. Błachowski, and P. Stoch, *Eur. J. Mineral.* 29, 63 (2017).
23. I. Jastrzębska, J. Szczerba, P. Stoch, A. Błachowski, K. Ruebenbauer, R. Prorok, and E. Śnieżek, *Nukleonika* 60, 47 (2015).
24. I. Barin, *Thermochemical Data of Pure Substances* (Weinheim: VCH Verlagsgesellschaft mbH, 1995).
25. X.W. Yang, A.P. He, and B.Z. Yuan, *The calculation handbook of high temperature aqueous solution thermodynamics data* (Beijing: Metallurgical Industry Press, 1983) (in Chinese).
26. R.O. Rihan and S. Nešić, *Corros. Sci.* 48, 2633 (2006).

Publisher's Note Springer Nature remains neutral with regard to jurisdictional claims in published maps and institutional affiliations.